Research Square

Preprints are preliminary reports that have not undergone peer review.
They should not be considered conclusive, used to inform clinical practice,
or referenced by the media as validated information.

Experimental and numerical investigation of an internally pinned externally finned compact cooler for high power density shearer ranging arms

Li Qingliang[1]

liqlzmkg@163.com

China University of Mining and Technology

Yu Ying[3]

Shanghai Tiandi Ming Equipment Technology Co., Ltd

Zhao Zeyuan[2]

Lanzhou University of Technology

Zhang Dong[2]

Lanzhou University of Technology

Cheng Gang[1]

China University of Mining and Technology

Research Article

Keywords:

Posted Date: November 11th, 2026

DOI: https://doi.org/10.21203/rs.3.rs-11130380/v1

License: This work is licensed under a Creative Commons Attribution 4.0 International License.
Read Full License

Additional Declarations: No competing interests reported.

Experimental and numerical investigation of an internally pinned externally finned compact cooler for high power density shearer ranging arms

Li Qingliang[1,3*], Yu Ying[3], Zhao Zeyuan[2], Zhang Dong[2], Cheng Gang[1]

HIGHLIGHT:

1. A compact internally pinned–externally finned cooler is developed.
2. The compound structure enhances heat transfer on both fluid sides.
3. The equivalent heat transfer coefficient increases by up to 50.46%.
4. Experiments and CFD clarify the pin-induced heat transfer enhancement mechanism.

Abstract: With the sharp increase in power density of shearer ranging arms used in thin coal seam mining, frequent failures due to overheating in the ranging arm gearbox have become a critical issue. As the core component for heat dissipation in the ranging arm, the heat transfer performance of the cooler is crucial for suppressing high temperature failures. Owing to the complex underground working environment and limited installation space, the key challenge lies in effectively enhancing cooling performance without altering the existing cooler dimensions and installation configuration. To address this, this paper proposes a high efficiency internally pinned and externally finned cooler. This cooler utilizes a pin structure within a small diameter tube and optimizes the external fin structure and layout, successfully resolving the conflict between efficient heat dissipation and structural size constraints within a limited space. Furthermore, the heat transfer enhancement mechanism of the pin structure is revealed, and its disturbing effect on the flow is analyzed. The pin structure disrupts the thermal boundary layer and viscous sublayer of the flow, significantly improving the cooler's heat transfer performance. To validate the effectiveness of the new cooler, a comparative experimental platform was designed and constructed, and comparative experiments were conducted between the internally pinned externally finned cooler and the original cooler. The experimental results show that the heat transfer performance of the new cooler is significantly superior to that of the original cooler. Under stead state conditions with a cooling water flow rate of 0.28 kg/s, the average equivalent heat transfer coefficient of the new cooler reaches 2031.03 W/(m²·K), representing a 30.83% improvement over the original cooler. Under dynamic conditions, its average equivalent heat transfer coefficient is 1889.13 W/(m²·K), a 45.00% improvement, with an average heat transfer rate of 9.62 kW, which is 1.44 times that of the original cooler. CFD numerical simulation results agree with experimental data within an error of 6.91%, further verifying the intrinsic enhancement mechanism of the internally pinned externally finned cooler through boundary layer disturbance. This study provides a composite enhanced heat dissipation [1]solution for the thermal optimization of high power density shearer ranging arms in thin coal seams, with significant engineering application value and promotional prospects.

Keywords: Thin seam shearer ranging arm; High efficiency cooler; Internally pinned externally finned structure; Boundary layer; Enhanced heat transfer

*Corresponding author : liqlzmkg@163.com
[1] School of Mechanical and Electrical Engineering, China University of Mining and Technology, Xuzhou 221116, China;
[2] School of Energy and Power Engineering, Lanzhou University of Technology, Lanzhou 730050, China;
[3] Machinery Research Institute, Shanghai Tiandi Ming Equipment Technology Co., Ltd., Shanghai 200030, China

Introduction

With the increasing demand for high efficiency and high intensity coal mining, shearers used in thin coal seams are being developed toward higher power and more compact configurations.[1, 2] The ranging arm, as a key transmission and cutting component of a shearer, operates under prolonged heavy loads and severe mechanical impacts. The continuous increase in installed power within a restricted structural envelope inevitably leads to a substantial increase in power density. Under these conditions, heat generated by gear meshing, bearing friction, and lubricant shear is continuously transferred to the lubricating oil, resulting in a considerable rise in the thermal load of the ranging arm. Excessive oil temperature can reduce lubricant viscosity, accelerate oil degradation, and deteriorate the lubrication condition of gears and bearings, thereby increasing the risk of wear, scuffing, and thermal failure.[3, 4] Therefore, effective thermal management of high power density ranging arms has become an important prerequisite for maintaining the reliability and service life of thin seam shearers. The thermal coupling between the gear transmission system, lubricating oil, housing, and cooling system has also been identified as an important factor governing the temperature field of the ranging arm[5, 6].

The cooler is one of the principal components responsible for removing heat from the ranging arm. In the commonly adopted oil–water cooling configuration, the cooler is immersed in the lubricating oil region, while cooling water flows through the internal tubes and continuously removes heat from the tube wall.[7, 8] Consequently, the overall cooling capability depends on the coupled heat transfer processes on both the oil side and water side, as well as heat conduction through the tube wall. For thin seam shearers, however, the available installation space is severely constrained by the surrounding gears, bearings, housing, and coal flow requirements. Increasing the tube diameter or enlarging the external heat transfer structure is therefore difficult without modifying the existing mechanical configuration[9, 10]. The cooler must simultaneously satisfy requirements for compactness, pressure resistance, manufacturability, and high heat transfer capacity[11]. These constraints distinguish the thermal management problem of shearer ranging arms from conventional heat exchanger applications and make compact passive heat transfer enhancement particularly attractive.[12]

Passive heat transfer enhancement through surface modification or flow manipulation has been extensively investigated for compact heat exchangers[13]. Extended surfaces can increase the effective heat transfer area, whereas ribs, grooves, corrugations, inserts, and vortex generators can disturb the near wall flow, promote secondary motion, and repeatedly interrupt the development of the thermal boundary layer[13, 14]. Reviews of fin and tube heat exchangers have shown that geometric modification can substantially improve heat transfer performance, although the resulting increase in flow resistance must also be considered[15, 16]. In particular, vortex generators and ribbed structures can induce longitudinal vortices and secondary flow, increase turbulence intensity, and transport relatively cold bulk fluid toward the heated wall, thereby reducing the thermal resistance associated with the near wall region. Numerical investigations of internally ribbed tubes have further demonstrated that rib arrangement strongly influences the induced flow structure and the resulting balance between heat transfer enhancement and frictional loss[17, 18]. These studies provide a theoretical basis for introducing flow disturbing structures into the internal passage of compact cooling tubes.

Despite these advances, directly applying conventional enhancement techniques to the cooler of a thin seam shearer ranging arm remains challenging. Internal inserts such as twisted tapes can

substantially intensify mixing and enhance heat transfer, but they may also introduce considerable pressure loss and require additional pumping power[19]. Moreover, machining complex ribs or grooves inside a small diameter, pressure bearing steel tube can increase manufacturing difficulty and reduce structural reliability[20]. On the external side, increasing the heat transfer area through fins is an established approach, but external enhancement alone cannot effectively address the thermal resistance associated with the internal cooling water flow[21]. Therefore, under a fixed installation envelope, a compound enhancement strategy that simultaneously modifies the internal flow field and increases the external heat transfer area may provide a more suitable solution[22]. Previous studies have demonstrated the potential of combining different enhancement mechanisms, but most have focused on conventional heat exchangers rather than the highly constrained cooling environment of high power density shearer ranging arms[23, 24].

To address this problem, an internally pinned and externally finned cooler is developed in the present study while maintaining the original installation configuration. The internal pin structures are arranged within the cooling tube to generate flow separation, secondary vortices, and enhanced mixing, thereby disrupting the viscous and thermal boundary layers adjacent to the tube wall. Meanwhile, external aluminum fins increase the effective heat transfer area and facilitate radial heat spreading from the tube wall. The compound structure therefore acts on two different thermal resistance components: the internal pins primarily reduce the internal convective resistance, whereas the external fins increase the external heat transfer capacity. Such a configuration is particularly suitable for compact cooling systems where enlarging the overall installation envelope is impractical. The objective of this study is to systematically evaluate the thermal performance and heat transfer enhancement mechanism of the proposed cooler. First, a comparative experimental platform is established to investigate the heat transfer performance of the original and enhanced coolers under both steady state and dynamic thermal conditions. Second, CFD simulations are conducted to characterize the internal flow field, local convective heat transfer coefficient, and temperature distribution, thereby clarifying how the pin structures modify the flow and thermal boundary layers. Finally, the numerical and experimental results are combined to establish the relationship between structural enhancement, flow field modification, thermal resistance reduction, and overall cooling performance. The logical relationship diagram of this study is shown in Figure 1. The resulting analysis provides a component level thermal management strategy for high power density shearer ranging arms and offers a basis for developing compact, high efficiency cooling structures for other space constrained heavy duty machinery.

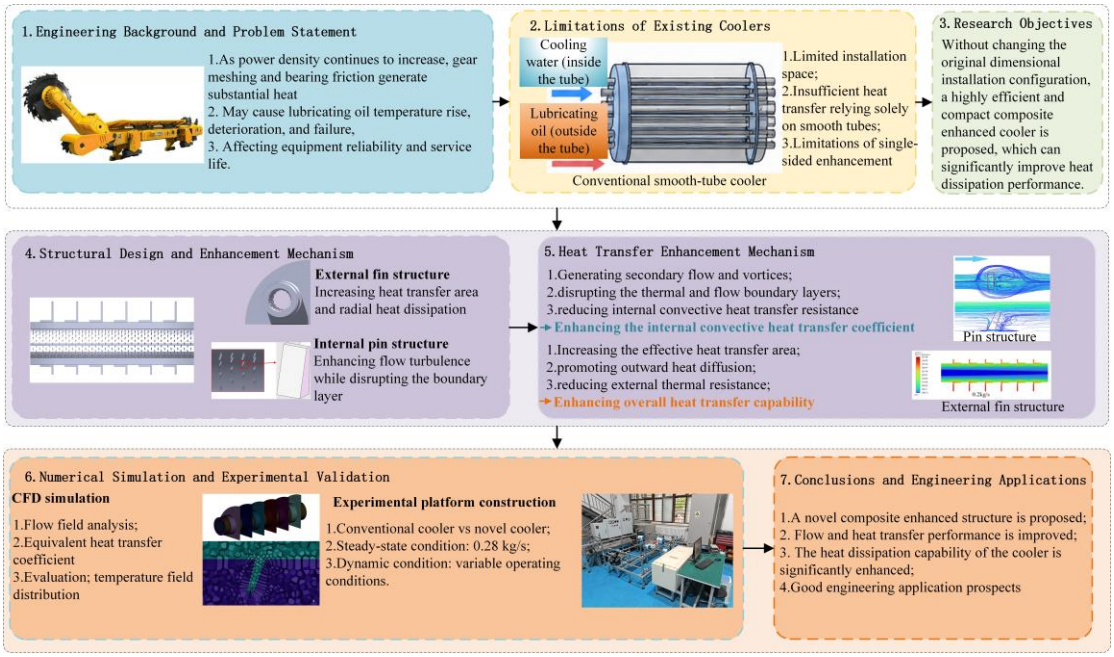


Fig. 1 Logical relationship diagram of the research

1 Cooler Structural Design and Experimental System Construction

1.1 Structural Design of the Internally Pinned Externally Finned Cooler

The original cooler currently used in thin seam shearer ranging arms is shown in Fig. 2(a). The cooler consists of four steel pipes and two water end connectors, typically installed in a dedicated mounting cavity on the side or rear of the ranging arm housing. The four steel pipes are connected to the external high pressure cooling water circuit through cast water end connectors at both ends and rigidly fixed to the ranging arm housing by bolts and seals. During operation, the tube bundle is submerged in or in close contact with the lubricating oil flowing through the housing. Its installation position and external envelope dimensions are strictly designed to avoid any kinematic interference with internal high speed rotating gears, bearings, and other transmission components.

Owing to the extremely limited installation space reserved for the cooler in the ranging arm gearbox, the cooling tube diameter cannot be too large, and the cooler must have a certain pressure bearing capacity. Therefore, to enhance the heat transfer coefficient on the inner wall of the cooler tube, double sided enhancement—both inside and outside the tube—must be implemented on steel pipes with an inner diameter of only 10 mm.

The internally pinned externally finned cooler designed and fabricated in this study is shown in Fig. 2(b). While maintaining the same installation method and interface configuration as the original cooler, a pin structure is designed and machined on the inner wall of the tube, and four passage aluminum alloy fins are designed and installed on the outer wall. The total length of the internally pinned externally finned cooler is 1262 mm, with a cooling tube length of 1110 mm, inner diameter of 12 mm, and outer diameter of 18 mm. The original cooler has a total length of 1262 mm, inner diameter of 16 mm, and outer diameter of 18 mm. The water end connector diameter for both coolers is 68 mm, and each tube installation hole has a diameter of 18 mm.

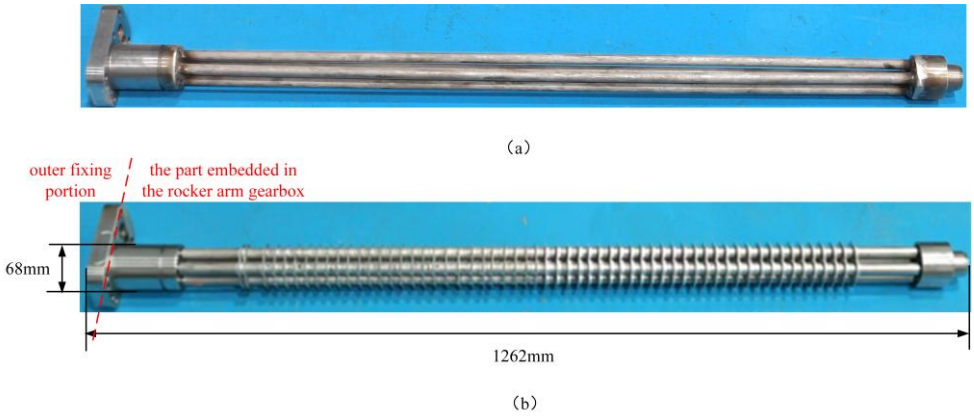


Fig. 2 Photographs of the coolers. (a) Original cooler; (b) Internally pinned externally finned cooler

To simultaneously maintain the pressure bearing capacity of the tube and achieve internal enhancement, a pin structure suitable for slender tubes was designed and machined, as shown in Fig. 3. The pins are machined sequentially using a slender milling cutter. Each pin is approximately 1 mm in height, arranged in staggered rows, with 16 pins evenly distributed around the circumference. In the flow direction, the circumferential rows are spaced 2 mm apart. Fifty four circular aluminum alloy fins are uniformly distributed on the outer surface of the tube. The fins have a diameter of 68 mm, thickness of 1 mm, and a 7 mm curl, and are made of 1017 aluminum alloy, installed sequentially on the outer wall of the four stainless steel tubes using a specially developed fixture.

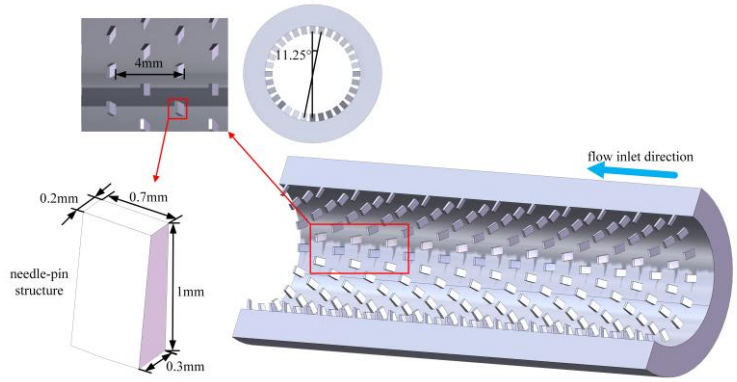


Fig. 3 Schematic diagram of internal pipe structure of the internally pinned externally finned cooler

The newly designed cooler adopts an internally pinned externally finned enhanced structure to optimize the cooler design. By adding external fins to increase the external heat transfer area, and by incorporating longitudinal vortex generators inside the tube to enhance mixing of cold and hot fluids in the vortex region—that is, disrupting the flow and thermal boundary layers—heat transfer is intensified. By adjusting design variables such as fin height and spacing on the outer wall, and pin length and diameter on the inner wall, optimal heat transfer performance is achieved while satisfying constraints on volume, material, and processing.

In actual ranging arm operation, heat generated by gear meshing and other sources is absorbed by the lubricating oil, forming a high temperature oil flow. This oil flows past the outer wall of the

cooler tube through splashing or gear agitation, transferring heat to the metal tube wall. Meanwhile, cooling water from the underground water supply system flows inside the tube, continuously carrying away the heat from the tube wall, thereby cooling the lubricating oil. The new cooler designed in this study is precisely intended to compoundly enhance this "oil side – tube wall – water side" heat transfer process.

1.2 Experimental System Construction

To test the actual cooling performance of the internally pinned externally finned cooler, an experimental system platform for cooler heat transfer performance testing was constructed. The system equipment connection diagram is shown in Fig. 4. The experimental system mainly consists of a cooling water tower, cooling water tank, circulating water pump, electromagnetic flow meter, pressure sensor, temperature sensor, test section, and data acquisition unit. A photograph of the experimental system is shown in Fig. 5. The experimental instruments and their accuracies are listed in Table 1.

Table 1 Model and accuracy of experimental instruments

Instrument	Model	Range	Accuracy
Pressure sensor	24A 17921	0 0.8MPa	0.2%FS
Temperature sensor	PT100	0 150℃	±0.15℃
Flow meter	NJLDB DN15mm	0.4 5m^3/h	0.5%
Data acquisition unit	DAQ34970	\	0.004%
Circulating pump	JET 1100S	1kW	\
DC power supply	UTP1306S	0~32V, 0~6A	≤0.1%+10mV, ≤0.2%+3mA
Heating pipe	Stainless steel single head	0.25 4kW	\

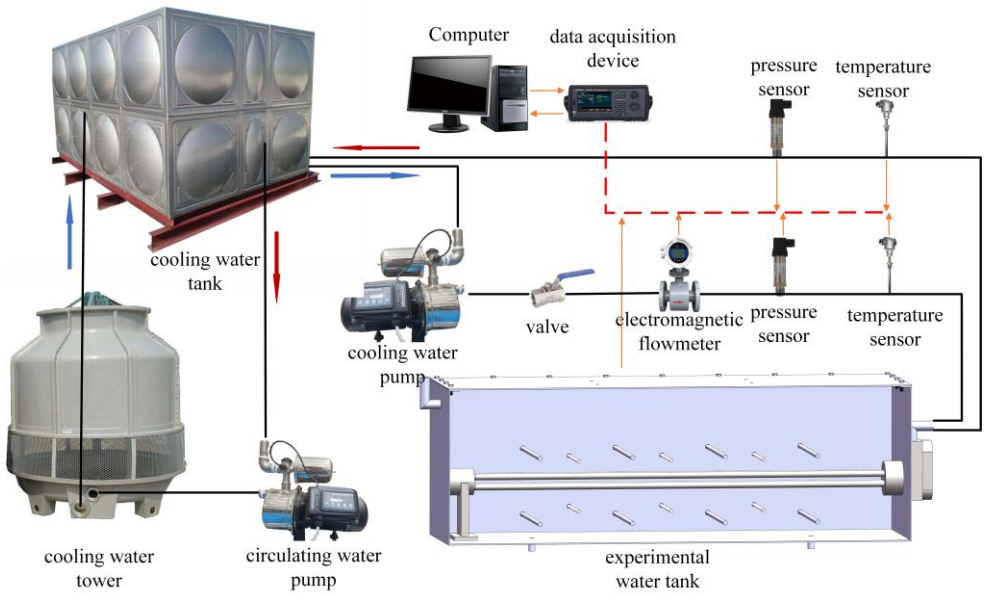


Fig. 4 Schematic diagram of the experimental system

During the experiment, cooling water is cooled by the cooling tower to approximately 15 °C

and stored in the cooling water tank. The cooling water is driven by the cooling water pump into the pipes, with flow rate controlled by valves. After passing through the electromagnetic flow meter, pressure sensor, and temperature sensor, the water enters the cooler located in the experimental water tank. After completing the circulation in the cooler, it returns to the cooling water tank through the cooler outlet.



Fig. 5 Photograph of the experimental platform for cooler heat transfer performance testing

The internal structure of the test section is shown in Fig. 6. Eight electric heating rods, each with a heating power of 2500 W, are uniformly distributed around the cooler in the water tank. Six temperature sensors are installed inside the tank, uniformly distributed on the upper and lower sides of the cooler, with probes positioned at the center of the tank to accurately measure the average temperature inside the experimental water tank. The cooler is fixed to the connector on the side wall of the experimental tank by bolts and seals, with the other end placed on a support base for stability.

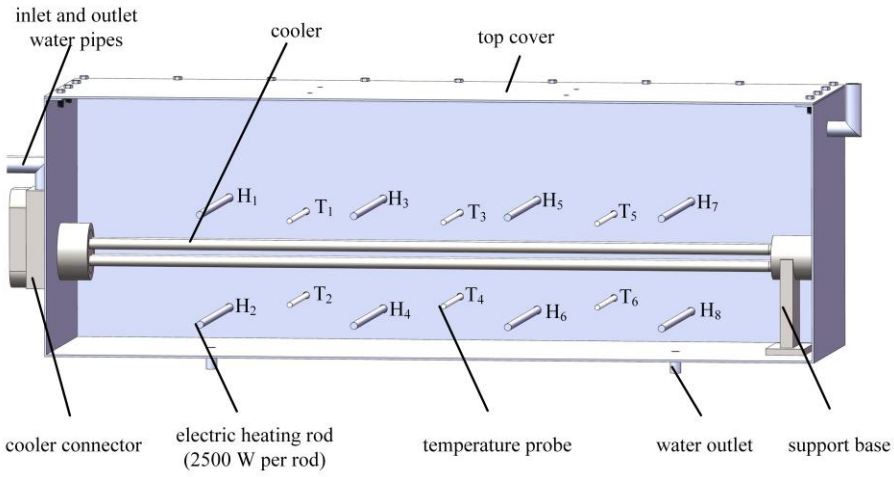


Fig. 6 Schematic diagram of the test section structure

1.3 Evaluation Indices for Cooler Heat Transfer Performance

The equivalent heat transfer coefficient k is an important indicator for evaluating heat exchanger performance, representing the amount of heat transferred per unit area per unit time.

$$k = \frac{\Phi}{A_i \times \Delta T_m} \tag{1}$$

where k is the equivalent heat transfer coefficient, W/(m²·K); Φ is the heat transfer rate of the cooler, kW; A_i is the inner surface area of the cooling tube, m²; ΔT_m is the logarithmic mean temperature

difference, °C.

The heat transfer rate is calculated as:

$$\Phi = c_p q_{\mathrm{m}} \Delta T_{\mathrm{w}} \tag{2}$$

where c_p is the specific heat capacity of water at constant pressure, kJ/(kg·K); q_{m} is the mass flow rate of cooling water, kg/s; ΔT_{w} is the temperature difference between cooling water inlet and outlet, °C.

$$\Delta T_{\mathrm{w}} = T_{\mathrm{out}} - T_{\mathrm{in}} \tag{3}$$

where T_{out} is the cooler outlet water temperature and T_{in} is the cooler inlet water temperature, °C.

The heat transfer temperature difference is expressed as the difference between the average temperature inside the experimental tank and the average of the cooling water inlet and outlet temperatures.

$$\Delta T_{\mathrm{m}} = \overline{T_{\mathrm{W}}} - \frac{T_{\mathrm{out}} + T_{\mathrm{in}}}{2} \tag{4}$$

The average temperature inside the experimental tank is calculated as:

$$\overline{T_{\mathrm{W}}} = \frac{1}{n}\sum_{i=1}^{\mathrm{n}} T_i \tag{5}$$

where T_i is the temperature measured at each of the six measurement points in the tank, °C, and n = 6.

To facilitate the comparison of the k value difference between the original cooler and the internally pinned externally finned cooler, $\overline{k_{\mathrm{I}}}$ and $\overline{k_{\mathrm{II}}}$ are introduced and calculated as follows:

$$\overline{k_{\mathrm{I}}} = \frac{1}{n}\sum_{i=1}^{\mathrm{n}} k_i \tag{6}$$

$$\overline{k_{\mathrm{II}}} = \frac{1}{n}\sum_{j=1}^{\mathrm{n}} k_j \tag{7}$$

where $\overline{k_{\mathrm{I}}}$ is value of the original cooler over a 10 minute steady state test, and $\overline{k_{\mathrm{II}}}$ is the average of the internally pinned externally finned cooler under the same conditions.

1.4 Experimental Uncertainty Analysis

To ensure the accuracy of experimental measurements, an uncertainty analysis was conducted. The key parameter characterizing the cooler is the equivalent heat transfer coefficient k. Based on the instrument accuracies listed in Table 1, the maximum relative error of the equivalent heat transfer coefficient, calculated by the error propagation principle, is 8.3%.

2 Numerical Simulation and Mechanism Analysis

To reveal the enhancement mechanism of the pin and fin structures, CFD numerical simulation of the internally pinned externally finned cooler was performed. Owing to the fine scale of the pin structure, accurate calculation requires a large number of mesh elements near the inner wall,

significantly increasing computation time. Since the cooler is highly symmetric, a local 100 mm long section was selected for CFD simulation to reveal its heat transfer enhancement mechanism.

2.1 Physical Model and Governing Equations

The physical model for numerical simulation is shown in Fig. 7. The model length is 100 mm. The original cooler has an inner diameter of 16 mm and outer diameter of 18 mm. The dimensions of the internally pinned externally finned cooler are shown in Fig. 8. The inner diameter is 10 mm, outer diameter is 18 mm, pin height is 1 mm, pin width is 0.7 mm, top thickness is 0.2 mm, and bottom thickness is 0.3 mm. Sixteen pins are arranged per circumferential row, with rows spaced 2 mm apart. The pins are inclined at 75° in the flow direction. Convective boundary conditions are applied to the outer tube wall and fin surfaces. The tube inlet is set as a velocity inlet, with cooling water mass flow rates of 0.52 kg/s, 0.44 kg/s, 0.36 kg/s, 0.28 kg/s, and 0.20 kg/s, and the outlet is set as a pressure outlet. Material properties used in the simulation are listed in Table 2.

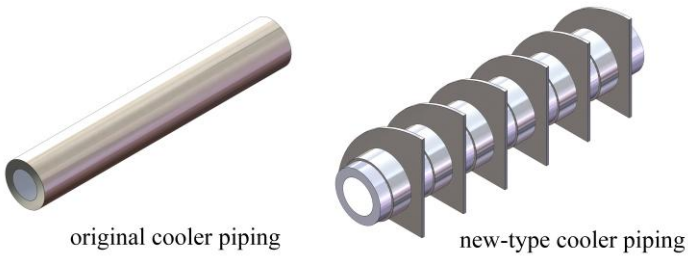


Fig. 7 Geometric models of the original cooler and the internally pinned externally finned cooler

Table 2 Material properties

Material	Thermophysical properties	Aluminum	Water	Stainless steel
Thermal conductivity	λ (W·m^{-1}·K^{-1})	230	0.6	21
Specific heat capacity	c_p (J·kg^{-1}·K^{-1})	871	4181.72	500
Specific heat	μ (Pa·s)	/	8.8937×10^{-4}	/
Density	ρ (kg·m^{-3})	2719	998.2	7930

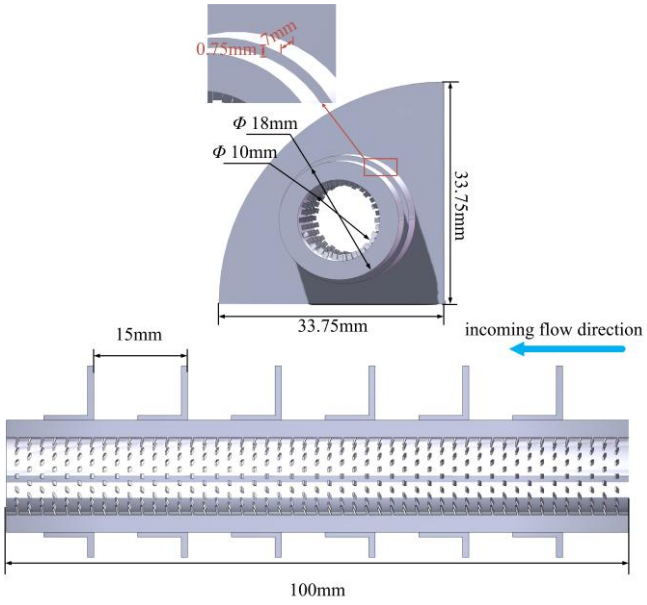


Fig. 8 Geometric dimensions of the internally pinned externally finned cooler for numerical

simulation

2.2 Numerical Simulation Validation

The energy conservation equations for the cooling pipe and fins are:

$$\rho c_p \frac{\partial T}{\partial t} = \lambda \nabla^2 T \tag{8}$$

where ρ is the fluid density, kg/m³; c_p is the fluid specific heat, kJ/(kg·K); T is the fluid temperature, K; λ is the fluid thermal conductivity, W/(m·K); and t is time, s.

The energy conservation equation for cooling water is:

$$\frac{\partial T}{\partial t} + v\nabla T = \frac{\lambda}{\rho c_p} \nabla^2 T \tag{9}$$

where v is the velocity vector of the cooling water.

The mass and momentum conservation equations for cooling water are:

$$\nabla \cdot \boldsymbol{v} = 0 \tag{10}$$

$$\rho\left(\frac{\partial \boldsymbol{v}}{\partial t} + \boldsymbol{v} \cdot \nabla \boldsymbol{v}\right) = -\nabla p + \mu \nabla^2 \boldsymbol{v} \tag{11}$$

where μ is the dynamic viscosity of the fluid, Pa·s.

The surface convective heat transfer coefficient is calculated as:

$$h = \frac{q}{A\Delta T} \tag{12}$$

where h is the convective heat transfer coefficient, W/(m²·K); q is the total heat transfer rate, W; A is the heat transfer area, m²; and ΔT is the temperature difference between the tube wall and cooling water, K.

The Reynolds number Re for internal flow is calculated as:

$$\mathrm{Re} = \frac{\rho U_\infty L}{\mu} \tag{13}$$

where $U\infty$ is the mainstream velocity in the tube, m/s, and L is the characteristic length of the tube, m.

According to the calculations, the Reynolds number at the lowest flow rate is approximately 17,000, indicating turbulent flow. Therefore, the k epsilon turbulence model was used in the simulation.

2.3 Numerical Simulation Validation

To validate the accuracy of the simulation results, the experimental results were compared with the numerical simulation results, as shown in Table 3. At a cooling water mass flow rate of 0.28 kg/s, the error in k for the original cooler is 3.24%, and for the internally pinned externally finned cooler is 6.25%. At a flow rate of 0.20 kg/s, the error for the original cooler is 1.61%, and for the new cooler is 6.91%. All relative errors are within 10%.

Table 3 Comparison of simulated and experimental results

q_m(kg/s)	Experimental results		Simulated results		Relative error	
	$\overline{k_I}$ (W·m^{-2}·K^{-1})	$\overline{k_{II}}$ (W·m^{-2}·K^{-1})	$\overline{k_I}$ (W·m^{-2}·K^{-1})	$\overline{k_{II}}$ (W·m^{-2}·K^{-1})	$\overline{k_I}$	$\overline{k_{II}}$
0.28	1552.39	2031.03	1503.05	1904.16	3.24%	6.25%
0.2	1456.53	1991.93	1433.01	1854.22	1.61%	6.91%

2.4 Analysis of Heat Transfer Enhancement Mechanism

2.4.1 Effect of Pin Structure on Flow

Fig. 9 shows the streamline distribution around a single pin. Upstream of the flow, the pin obstructs the water flow: water above passes over the top, while water below is directed toward the pin root before passing around both sides. This disturbance introduces lower temperature cooling water from the mainstream to the near wall region, effectively breaking the flow and thermal boundary layers and reducing viscous sublayer thickness. Convective heat transfer becomes dominant, increasing the heat transfer coefficient. The high temperature water near the wall is replaced by lower temperature mainstream water, increasing the heat transfer temperature difference and improving heat exchange efficiency. Thus, the internally pinned externally finned cooler enhances heat transfer by incorporating longitudinal vortex generators (i.e., pin structures) inside the tube, which intensify mixing of cold and hot fluids in the vortex region by disrupting the flow and thermal boundary layers.

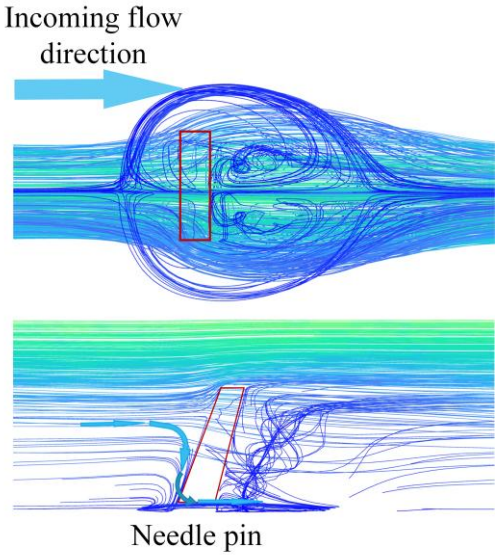


Fig. 9 Streamline distribution around a single pin.

2.4.2 Effect of Pin Structure on Convective Heat Transfer Coefficient

Fig. 10 shows the local inner wall convective heat transfer coefficient of the internally pinned externally finned cooler. Owing to the flow disturbance caused by the pins, it can be observed that the convective heat transfer coefficient in front of and on the sides of the pins is higher than in regions without pins, indicating a significant enhancement effect of the pins on internal flow heat transfer. However, due to flow obstruction by the pins, a small region behind each pin exhibits a slightly lower local convective heat transfer coefficient because of reduced local flow velocity.

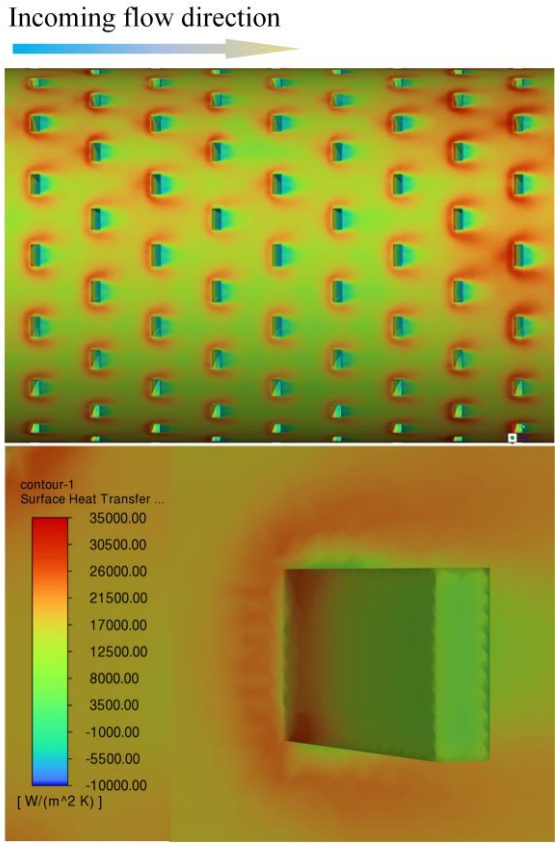
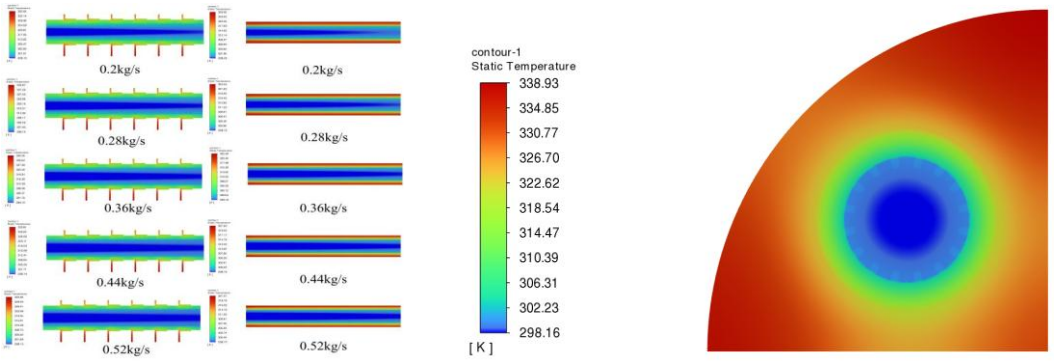


Fig. 10 Local inner wall convective heat transfer coefficient of the internally pinned externally finned cooler.

2.4.3 Temperature Distribution in Heat Transfer Regions

Fig. 11 shows the temperature distribution contours of the two cooler types at different flow velocities. It can be observed that at the contact positions between the fins and the tube wall in the internally pinned externally finned cooler, the temperature is higher than at the water convecting surface, indicating that more heat is conducted through the fins to the tube wall, thereby improving overall heat transfer performance. As flow velocity decreases, the region of heated cooling water gradually expands. Since the central cooling water velocity in the new cooler is higher than in the original cooler, the proportion of heated water region is smaller. In addition to the enhanced heat transfer efficiency caused by flow disturbance as mentioned above, the pins themselves also increase the heat transfer area, further increasing the heat transfer rate. The fin temperature contour in Fig. 11(b) shows that the fin structure effectively diffuses wall heat radially outward, indicating that the fins not only increase the heat dissipation area but also help conduct heat from local hot spots laterally. At the component level, this mechanism contributes to improving the temperature distribution uniformity within the cooler itself, offering a potential approach for homogenizing the temperature field in key areas of the ranging arm at the system level.



(a) (b)

Fig. 11 (a) Temperature distribution contours of the internally pinned externally finned cooler and original cooler; (b) Temperature contour of the fins in the internally pinned externally finned cooler.

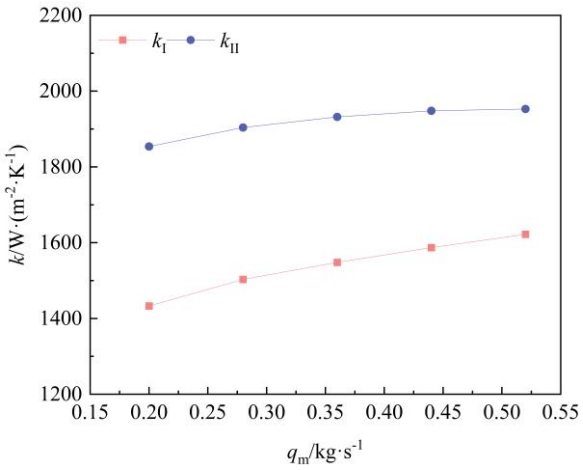


Fig. 12 Numerical simulation results of heat transfer coefficient for the coolers.

3 Cooler Performance Testing

To evaluate the cooler performance under operating conditions simulating the actual thermal environment of the ranging arm, the cooler performance tests were closely aligned with its engineering application context:

(1) Steady state condition tests: The experimental tank temperature was maintained at a constant 80 °C, simulating the typical operating state when the ranging arm reaches thermal equilibrium during prolonged continuous heavy load cutting. In this state, the cooler performance determines the steady state operating temperature level of the system.

(2) Dynamic condition tests: The tank temperature was allowed to cool naturally from 90 °C to 40 °C, simulating the cooling recovery process when the ranging arm enters light load, idle, or shutdown states after experiencing peak loads. This process assesses the cooler's ability to suppress peak temperature rise and accelerate heat dissipation, which is critical for thermal inertia and the sustainability of intermittent operations.

3.1 Steady State Heat Transfer Performance Tests

To compare the performance difference between the original cooler and the internally pinned externally finned cooler at different cooling water flow rates, steady state heat transfer performance

experiments were conducted. Fig. 13 shows the temporal variation of heat transfer coefficient for the two coolers at approximately 80 °C constant temperature, under mass flow rates of 0.20 kg/s and 0.28 kg/s.

From Fig. 13, it can be seen that under the same operating condition (80 °C constant temperature, different cooling water flow rates), the heat transfer coefficient (k) of the internally pinned externally finned cooler is significantly higher than that of the original cooler, and both coolers show improved heat transfer performance with increasing cooling water flow rate. The heat transfer coefficient of the new cooler is considerably higher than that of the original cooler, because the internal pin structure creates additional turbulence, disrupting the flow boundary layer between the fluid and tube wall and reducing convective thermal resistance. Additionally, the external fins increase the external heat transfer area, further enhancing the cooler's heat transfer performance.

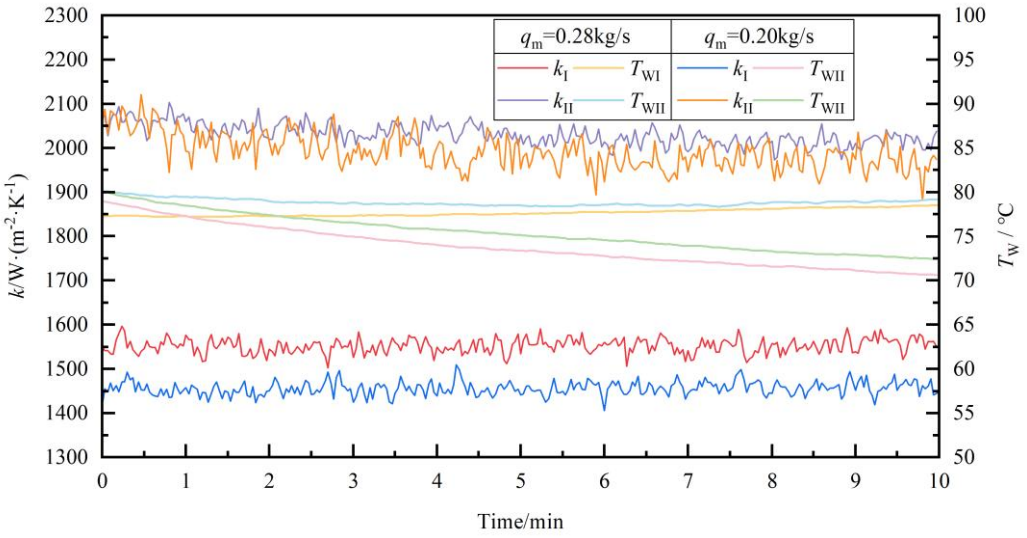


Fig. 13 Performance testing of the two coolers under steady state conditions.

3.2 Dynamic Heat Transfer Performance Tests

To evaluate the heat transfer performance of the internally pinned externally finned cooler at different temperatures, dynamic heat transfer performance tests were conducted. The heat transfer performance of the cooler during cooling from 90 °C to 40 °C was tested under cooling water flow rates of 0.20 kg/s and 0.28 kg/s. The results are shown in Fig. 14.

From Fig. 14, it can be observed that the heat transfer performance of the new cooler at 0.28 kg/s is slightly higher than at 0.20 kg/s. This is mainly because a higher cooling water flow rate results in lower cooling water temperature and a larger temperature difference, leading to a higher heat transfer coefficient. Additionally, as the tank temperature decreases, the k value of the cooler decreases accordingly, because the reduced temperature difference weakens the driving force for heat transfer. The heat transfer coefficient of the new cooler reaches a maximum of 2223.38 W/(m²·K) and remains above 1600 W/(m²·K) throughout the cooling process. Even when the external convective heat transfer coefficient weakens, it still outperforms the original cooler under steady state conditions. This indicates that increasing cooling water flow rate enhances heat transfer through a larger temperature difference, and the internally pinned externally finned structure maintains superior heat transfer performance even when the driving force is reduced as the tank temperature decreases, verifying its high efficiency and stability during dynamic cooling.

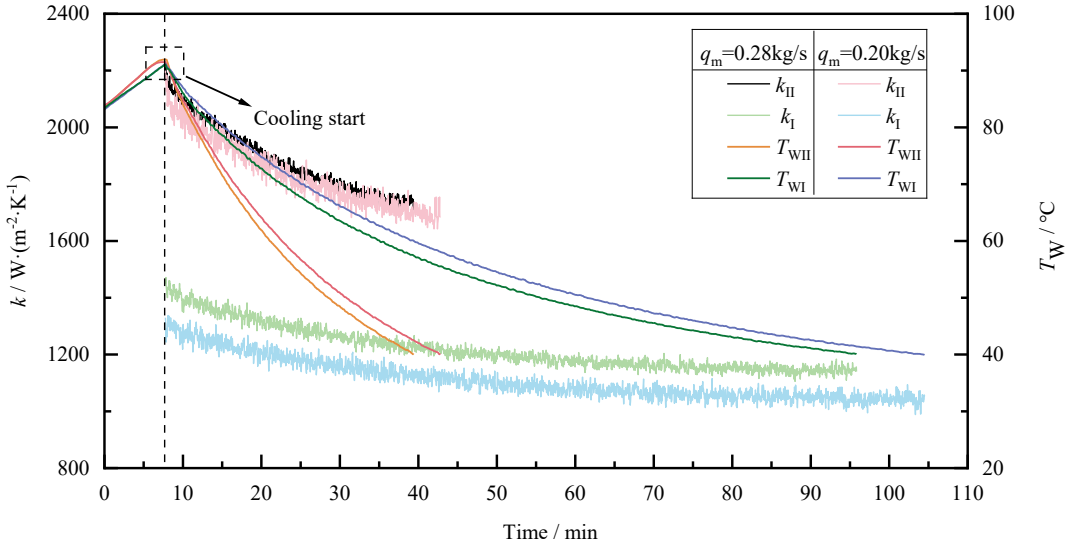


Fig. 14 Performance testing of the two coolers under dynamic conditions.

Fig. 15 shows the variation of heat transfer rate (Φ) of the coolers under dynamic conditions. It can be seen that the heat transfer rates of both coolers show an overall decreasing trend during the cooling process, and the heat transfer rate of the internally pinned externally finned cooler (Φ_{II}) always remains above that of the original cooler (Φ_I), indicating superior heat transfer performance. At a cooling water flow rate of 0.28 kg/s, the initial peak heat transfer rate of the new cooler is approximately 18.07 kW, significantly higher than that of the original cooler. The integrated area under the curve yields an average heat transfer rate of 9.62 kW, representing a 59% increase over the original cooler. At 0.20 kg/s, the initial peak heat transfer rate of the new cooler is approximately 14.91 kW, with an average of 8.17 kW, representing a 55% increase over the original cooler. Combined with the numerical simulation results, the internally pinned externally finned cooler enhances flow turbulence through the internal pin structure and external fins, increasing the heat transfer rate, and therefore its cooling rate is significantly higher than that of the original cooler.

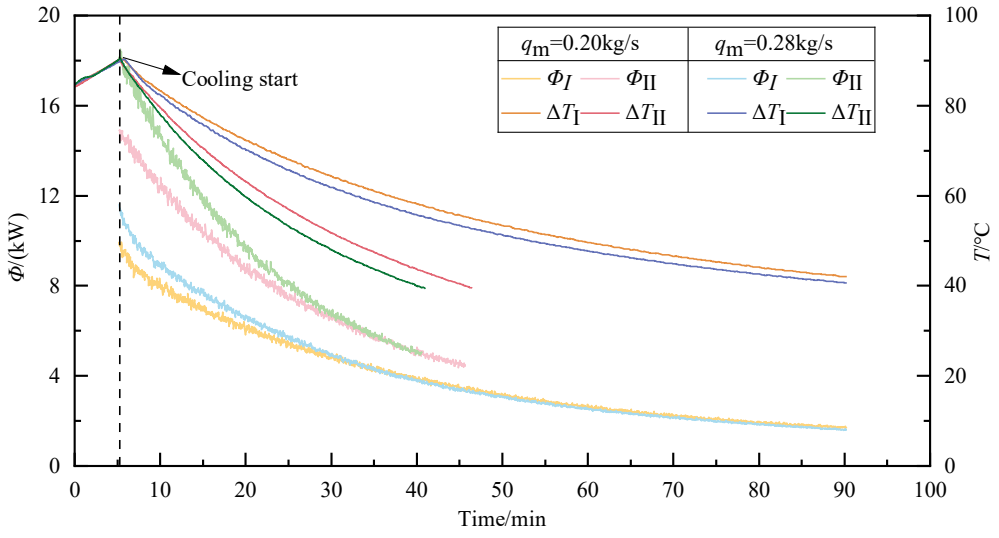


Fig. 15 Comparison of heat transfer rate of the two coolers under dynamic conditions.

3.3 Comprehensive Analysis of Heat Transfer Performance

Tables 4 and 5 summarize the average k values of the two coolers at cooling water flow rates of 0.28 kg/s and 0.20 kg/s under steady state and dynamic conditions, respectively. From both tables, it can be seen that the average k values of the internally pinned externally finned cooler are higher than those of the original cooler, confirming the positive effect of the internally pinned externally finned structure on heat transfer performance. The improvement under steady state conditions exceeds 30%, while under dynamic conditions it ranges from 45% to 50%.

Table 4 Comparison of average k of the two coolers under steady state conditions

q_m(kg/s)	$\overline{k}_{\mathrm{I}}$ (W·m^{2}·K^{1})	$\overline{k}_{\mathrm{II}}$ (W·m^{2}·K^{1})	Improvement (%)
0.28	1552.39	2031.03	30.83%
0.2	1456.53	1991.93	37.31%

Table 5 Comparison of average k of the two coolers under dynamic conditions

q_m(kg/s)	$\overline{k}_{\mathrm{I}}$ (W·m^{2}·K^{1})	$\overline{k}_{\mathrm{II}}$ (W·m^{2}·K^{1})	Improvement (%)
0.28	1302.98	1889.13	45.00%
0.2	1219.87	1835.44	50.46%

Comparing Tables 4 and 5, the improvement in k under dynamic conditions is greater. This is because during cooler operation, the main factors influencing the heat transfer coefficient are external convective thermal resistance, wall conduction thermal resistance, and internal convective thermal resistance. The wall conduction thermal resistance remains constant under both conditions. Under steady state conditions, the external convective thermal resistance is relatively stable, and the primary factor improving cooling performance is the reduction of internal convective thermal resistance, which the pin structure effectively achieves. Under dynamic conditions, the heating power varies continuously, reducing the temperature difference between the inside and outside of the tube, weakening the intensity of external natural convection and significantly increasing external convective thermal resistance. The external fin structure mitigates this increase in thermal resistance, while the internal pin structure reduces convective thermal resistance. Combined, these effects lead to the larger improvement in k under dynamic conditions.

Table 6 Comparison of average heat transfer rate of the two coolers under dynamic conditions

q_m (kg/s)	Q_{I} (kW)	Q_{II} (kW)	Improvement factor
0.28	3,95	9.62	1.44
0.20	3.64	8.15	1.24

Table 6 summarizes the average heat transfer rates of the coolers at 0.20 kg/s and 0.28 kg/s under dynamic conditions. The average heat transfer rate of the internally pinned externally finned cooler is higher than that of the original cooler for both flow rates. The maximum improvement factor reaches 1.44, further confirming that the pin structure and external fins enhance the cooler's heat transfer performance.

4 Conclusion, Industrial Applicability and Limitations

4.1 Conclusion

This paper proposes a high efficiency internally pinned externally finned cooler for high power

shearers in thin coal seams, innovatively designing and optimizing the external fin structure and layout to resolve the conflict between efficient heat dissipation and structural size constraints within a limited space. The enhancement mechanism of the pin structure within the cooler tube is revealed, clarifying its disturbing effect on the flow, which effectively breaks the thermal boundary layer and viscous sublayer, improving cooler performance. Through CFD numerical simulation and experimental performance testing, the following conclusions are drawn:

(1) At a cooling water flow rate of 0.28 kg/s, the average equivalent heat transfer coefficient of the new cooler under steady state conditions is 2031.03 W/(m²·K), and under dynamic conditions it is 1889.13 W/(m²·K).

(2) At the same cooling water flow rate, under both dynamic and steady state conditions, the equivalent heat transfer coefficient of the internally pinned externally finned cooler is higher than that of the original cooler, with improvements exceeding 30% in all cases.

(3) Under dynamic conditions, the average heat transfer rate of the new cooler at 0.28 kg/s is 9.62 kW, 1.44 times that of the original cooler.

(4) Comparison of CFD numerical simulation results and experimental data yields errors below 6.94%. The CFD simulation further confirms that the pin structure effectively breaks the flow and thermal boundary layers, enhancing the heat transfer capability of the cooler.

(5) Although this study did not directly test the temperature rise and temperature field of the complete ranging arm, the experimental and numerical results confirm the superior heat dissipation performance of the internally pinned externally finned cooler. The significant improvements in heat transfer coefficient and heat transfer rate provide a critical component level support for fundamentally improving the thermal state of high power density ranging arms. This study offers an efficient, directly replaceable heat dissipation upgrade solution for mitigating overheating risks in thin seam shearer ranging arms under heavy load and impact conditions, with significant engineering application value.

4.2 Industrial Applicability

The internally-pinned externally-finned cooler is fully consistent with the original cooler in terms of installation method, interface, and external dimensions, allowing direct replacement without modifying the ranging arm housing. This structure achieves dual-sided enhancement—internal boundary layer disturbance and external heat dissipation area expansion—without increasing the external dimensions, breaking through the bottleneck of single-sided enhancement in confined spaces without compromising the pressure-bearing capacity of the tube wall. The steady-state equivalent heat transfer coefficient is improved by 30.83%–37.31%, and the dynamic improvement reaches 45.00%–50.46%. The average heat transfer rate is 1.24–1.44 times that of the original cooler, and the discrepancy between experimental and CFD results is below 6.94%, demonstrating high engineering promotional value.

4.3 Limitations

This study only tested the cooler as an individual component and did not verify the temperature field improvement of the complete ranging arm. The pin structure requires multiple machining operations, increasing manufacturing cost and production cycle. Flow resistance and pump power consumption have not been systematically evaluated. Only cooling water was used as the working fluid, without investigating other fluids. The durability and scaling effects under long-term service conditions remain to be studied.

Statements and Declarations

Author contributions All authors contributed to the research conception and design. Experimental preparation, data acquisition, and analysis were carried out by Zhao Zeyuan. Zhang Dong and Li Qingliang provided assistance in methodology, formal analysis, and investigation. The first draft of the manuscript was written by Zhao Zeyuan. Yu Ying and Cheng Gang were responsible for supervision and guidance. All authors commented on previous versions of the manuscript. All authors read and approved the final manuscript.

Acknowledgements This work was supported by the National Natural Science Foundation of China (52275039).

References

[1]Sadeghianjahromi A, Wang C C. Heat transfer enhancement in fin and tube heat exchangers – A review on different mechanisms [J]. Renewable and Sustainable Energy Reviews, 2021, 137: 110470.

[2]Nadeem T B, Imran M, Arshad A, et al. Numerical investigation and optimization of finned tube heat exchanger for enhanced thermal hydraulic performance in IEC application [J]. Thermal Science and Engineering Progress, 2026, 76: 104805.

[3]Awais M, Bhuiyan A A. Heat transfer enhancement using different types of vortex generators (VGs): A review on experimental and numerical activities [J]. Thermal Science and Engineering Progress, 2018, 5: 524 545.

[4]Hu Y, Lu F, Ge W, et al. Research on the influence of structural parameters and optimization of heat sinks for high power helicopter intermediate gearboxes [J]. International Journal of Thermal Sciences, 2026, 219: 110237.

[5] Mao Jun, Zhu Yu, Chen Hongyue, et al. Solid thermal Coupling Analysis and Tooth Profile Modification of Shearer Rocker Arm Gears[J]. Journal of China Coal Society, 2017, 42(06): 1598 1606.

[6]Parey A, Jain N K, Koria S C. Failure analysis of air cooled condenser gearbox [J]. Case Studies in Engineering Failure Analysis, 2014, 2(2): 150 156.

[7]Zhang X, Ji Z, Wang J, et al. Research progress on structural optimization design of microchannel heat sinks applied to electronic devices [J]. Applied Thermal Engineering, 2023, 235: 121294.

[8]Zhang Y, Peng F, Jia H, et al. Conformal geometric design and additive manufacturing for special shaped TPMS heat exchangers [J]. International Journal of Heat and Mass Transfer, 2025, 247: 127146.

[9] Zhai Yusheng, Shi Chunxiang, Lü Xiao, et al. Development Status and Key Technologies of Drum type Shearers for Thin Coal Seams [J]. Coal Engineering, 2020, 52(7): 182 186.

Zhai Yusheng, Shi Chunxiang, Lü Xiao, et al. Development Status and Key Technologies of Drum type Shearer for Thin Coal Seams[J]. Coal Engineering, 2020, 52(07): 182 186.

[10] Li Xiaojun. Application of Cooling Systems and Devices for Shearer Ranging Arm Gearboxes [J]. Mechanical Management and Development, 2024, 39(11): 161 162-165.

[11]Sarmadian A, Moghaddam H A, Asnaashari A, et al. Flow boiling heat transfer and pressure drop characteristics of Isobutane in horizontal channels with twisted tapes [J]. International Journal of Heat and Mass Transfer, 2020, 162: 120345.

[12] Qin Chao, Wu Fan, Zhang Liang. Design of the Cooling System for Shearer Ranging Arms [J]. Scientific and Technological Innovation, 2021, (24): 31 32.

[13]Zheng N, Liu P, Shan F, et al. Effects of rib arrangements on the flow pattern and heat transfer in an internally ribbed heat exchanger tube [J]. International Journal of Thermal Sciences, 2016, 101: 93

105.
[14]Li Z, Wu Y, Tang G, et al. Numerical analysis of buoyancy effect and heat transfer enhancement in flow of supercritical water through internally ribbed tubes [J]. Applied Thermal Engineering, 2016, 98: 1080 1090.
[15]Li H Y, Liao W R, Li T Y, et al. Application of vortex generators to heat transfer enhancement of a pin fin heat sink [J]. International Journal of Heat and Mass Transfer, 2017, 112: 940 949.
[16]Kumar D, Dalal A. Effect of shear thinning fluid and position of curved rectangular winglet vortex generators on the performance of finned tube heat exchanger [J]. International Journal of Thermal Sciences, 2026, 229: 111128.
[17]Manglik R M, Bergles A E. Swirl flow heat transfer and pressure drop with twisted tape inserts [M] Advances in Heat Transfer. Elsevier. 2003: 183 266.
[18] Huang Shenjie, Xiong Tong, Wang Genfa, et al. Research Status and Prospects of Twisted Tape Inserts for Enhanced Boiling Heat Transfer in Tubes[J]. Journal of Refrigeration, 2022, 43(03): 45 56.
[19]Mahmoudi M, Goharkhah M, Hossainpour S, et al. Performance evaluation of a porous fin heat sink for electronic device thermal management: an experimental study [J]. Thermal Science and Engineering Progress, 2026, 75: 104737.
[20]He B, Li L, He G, et al. Experimental study on heat transfer performance of micro grooved I shaped aluminum heat pipe for heat pipe heat exchangers [J]. Applied Thermal Engineering, 2024, 253: 123773.
[21]Ji J, Ni X, Zhao J, et al. Numerical investigation of the effect of the structure and number of spiral baffles on the vibration and heat transfer coefficient of spiral tubes within spiral tube heat exchangers [J]. Applied Thermal Engineering, 2025, 258: 124545.
[22]Hodroj M, Al Takash A, Faraj J, et al. Finned tube heat exchangers: A comprehensive review and integrated CFD optimization framework with a normalized thermal hydraulic merit index [J]. International Communications in Heat and Mass Transfer, 2026, 172: 110379.
[23]Tychanicz Kwiecień M, Gil P. Experimental investigation of thermal and flow characteristics of a prototype minichannel heat exchanger [J]. International Journal of Heat and Mass Transfer, 2024, 231: 125825.
[24]Vargas B A d F, Kanizawa F T. Modeling and performance evaluation of crossflow microchannel heat exchangers for natural gas liquefaction systems [J]. Applied Thermal Engineering, 2026, 300: 131366.